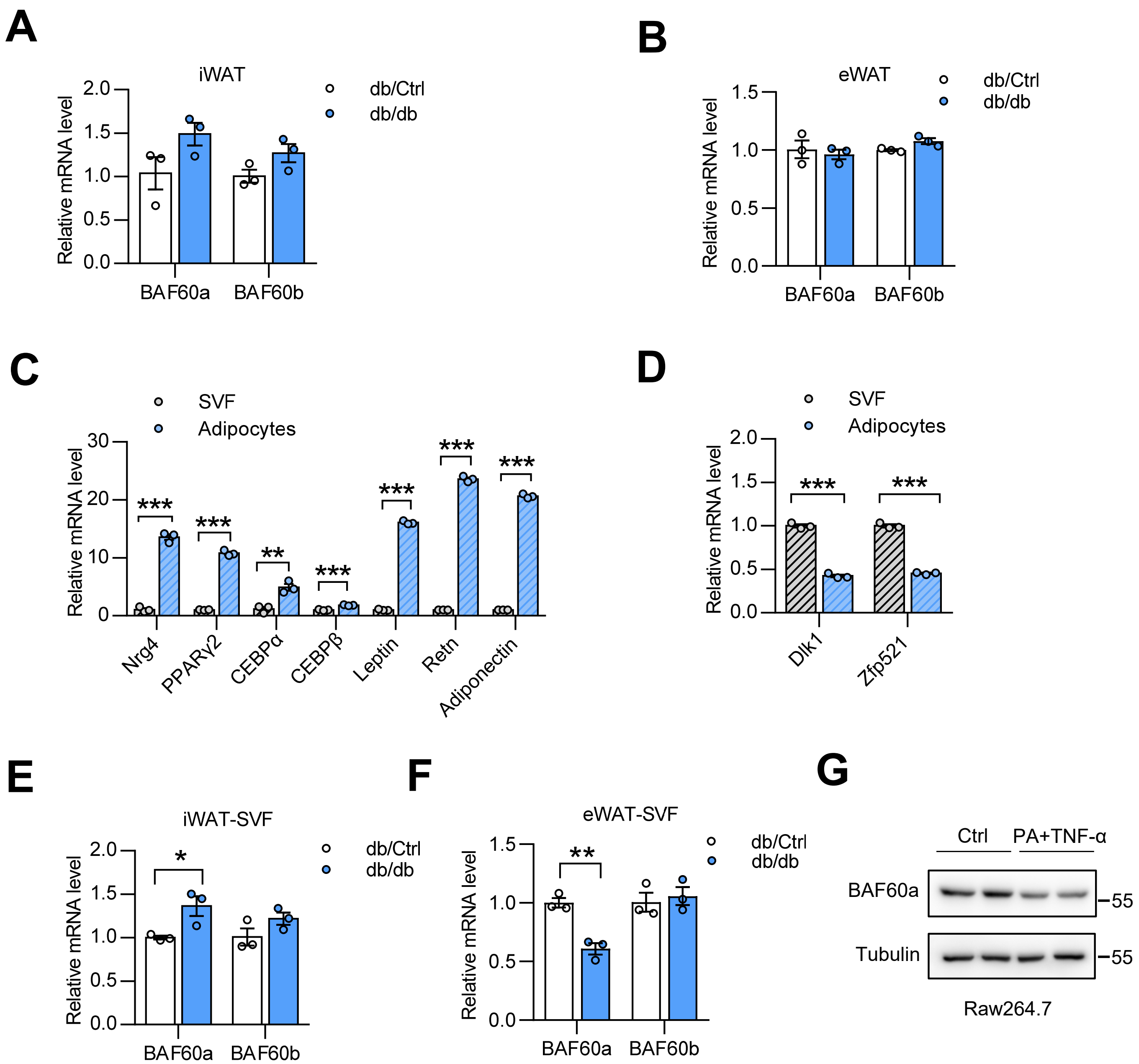

Supplementary Fig. 1. BAF60a and BAF60b gene expression in white adipose tissues and their SVFs from *db/db* and control mice.

(**A-B**) qPCR analysis of BAF60a and BAF60b mRNA expression in iWAT (**A**) and eWAT (**B**) obtained from control and *db/db* mice (n = 3). (**C-D**) qPCR analysis of mRNA expression of marker genes of adipocyte (**C**) and SVF (**D**) isolated from adipose tissue of WT mice (n = 3). (**E-F**) qPCR analysis of BAF60a and BAF60b mRNA expression in iWAT-SVF (**E**) and eWAT-SVF (**F**) from control and *db/db* mice (n = 3). **(G)** Western blots of BAF60a protein expression in PA (0.5 mM) and TNF-α (50 ng/mL)-treated RAW264.7 cells for 48 h. Data represent mean ± SEM. *$P < 0.05$, **$P < 0.01$, and ***$P < 0.001$.

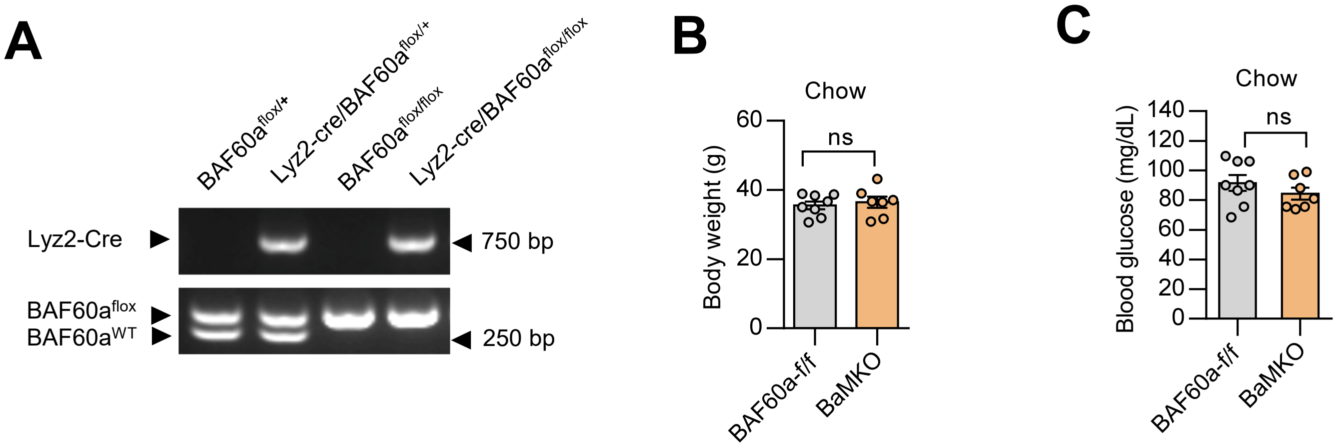

Supplementary Fig. 2. Generation and characterization of BaMKO mice on chow diet. (**A**) Genotyping of BaMKO mice. (**B-C**) Body weight (**B**) and fasting blood glucose levels (**C**) of control and BaMKO mice fed with chow diet for 20 weeks (n = 7-8). Data represent mean ± SEM. ns, no significance.

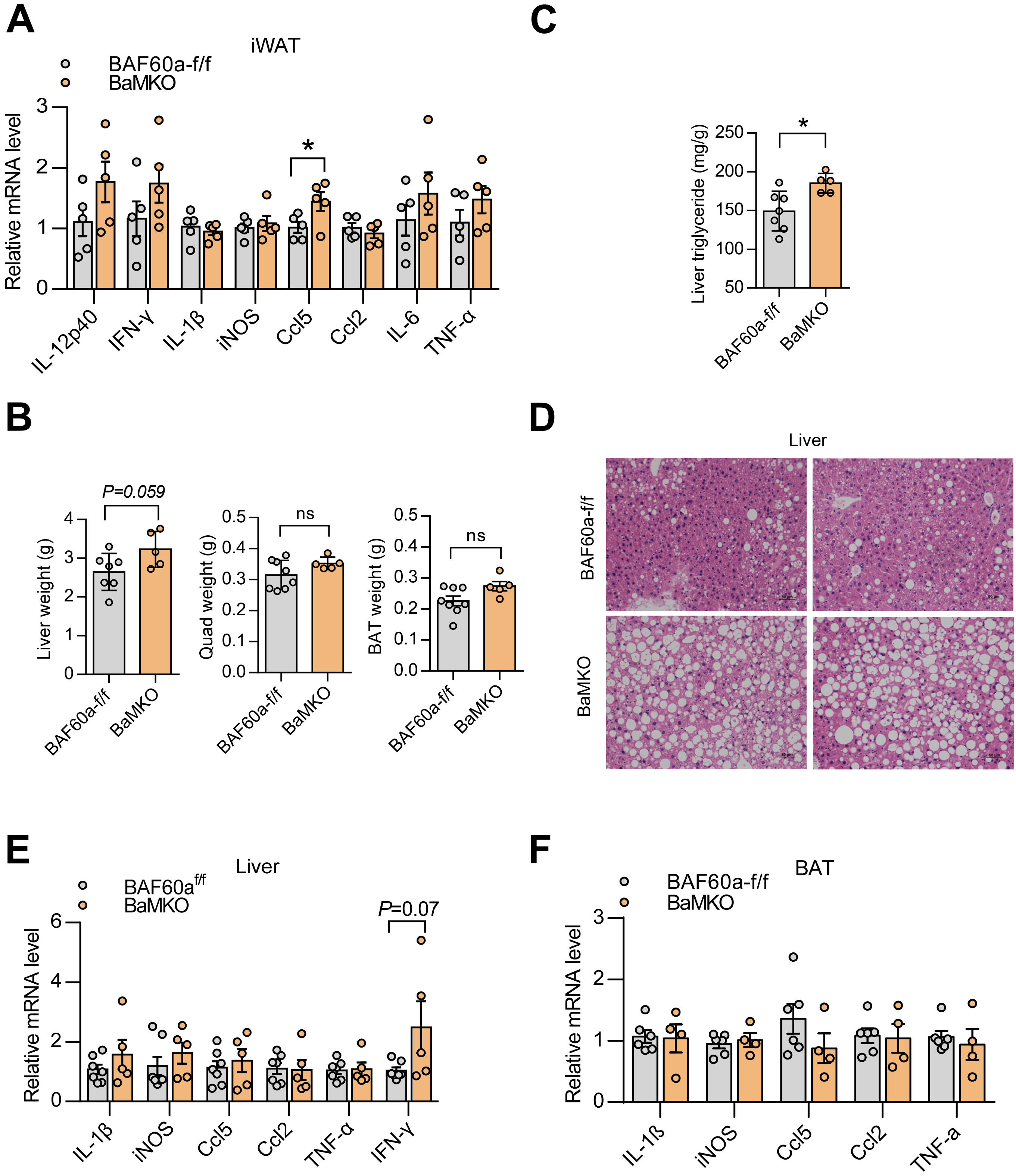

Supplementary Fig. 3. BaMKO exhibits a mild effect on liver and BAT inflammation in HFD-fed mice.

(**A**) qPCR analysis of pro-inflammatory genes in iWAT from BAF60a-f/f and BaMKO mice fed with HFD for 20 weeks (n = 5). (**B**) Tissue weight of liver, Quad and BAT obtained from BAF60a-f/f and BaMKO mice (n = 5-7). (**C**) Liver triglyceride (TG) content in BAF60a-f/f and BaMKO mice (n = 5-7). (**D**) Representative H&E staining images of liver sections from BAF60a-f/f and BaMKO mice. Scale bars: 50 µm. (**E-F**) qPCR analysis of proinflammatory genes in liver (**E**) (n = 5-7) and BAT (**F**) (n = 4-6) from BAF60a-f/f and BaMKO mice. Mice were fed with HFD for 16 weeks prior to tissue dissection and analysis. Data represent mean ± SEM. **P* < 0.05; ns, no significance.

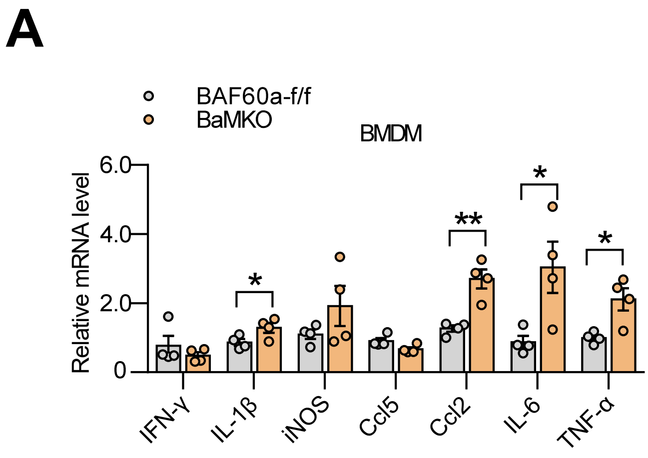

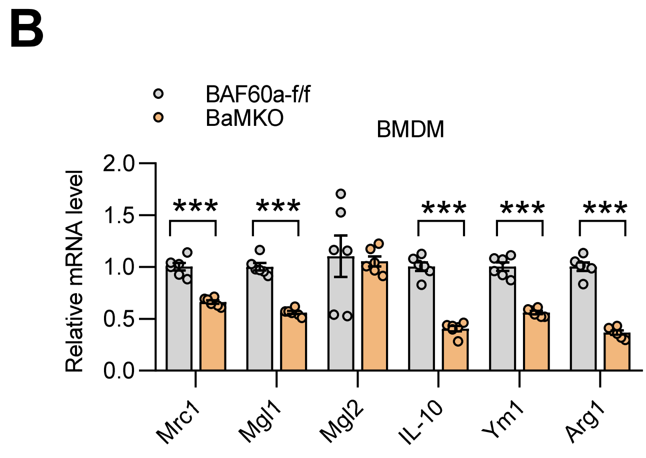

Supplementary Fig. 4. Myeloid-specific BAF60a inactivation modulates polarization and activation of bone-marrow-derived macrophages (BMDMs).

(**A-B**) BMDMs from BAF60a-f/f and BaMKO mice were stimulated with LPS (100 ng/mL) (n=4) (**A**) or IL-4 (20 ng/mL) (n=6) (**B**) for 24 h, the expression of M1 and M2-related genes were determined by qPCR. Data represent mean ± SEM. *$P < 0.05$, **$P < 0.01$ and ***$P < 0.001$; ns, no significance.

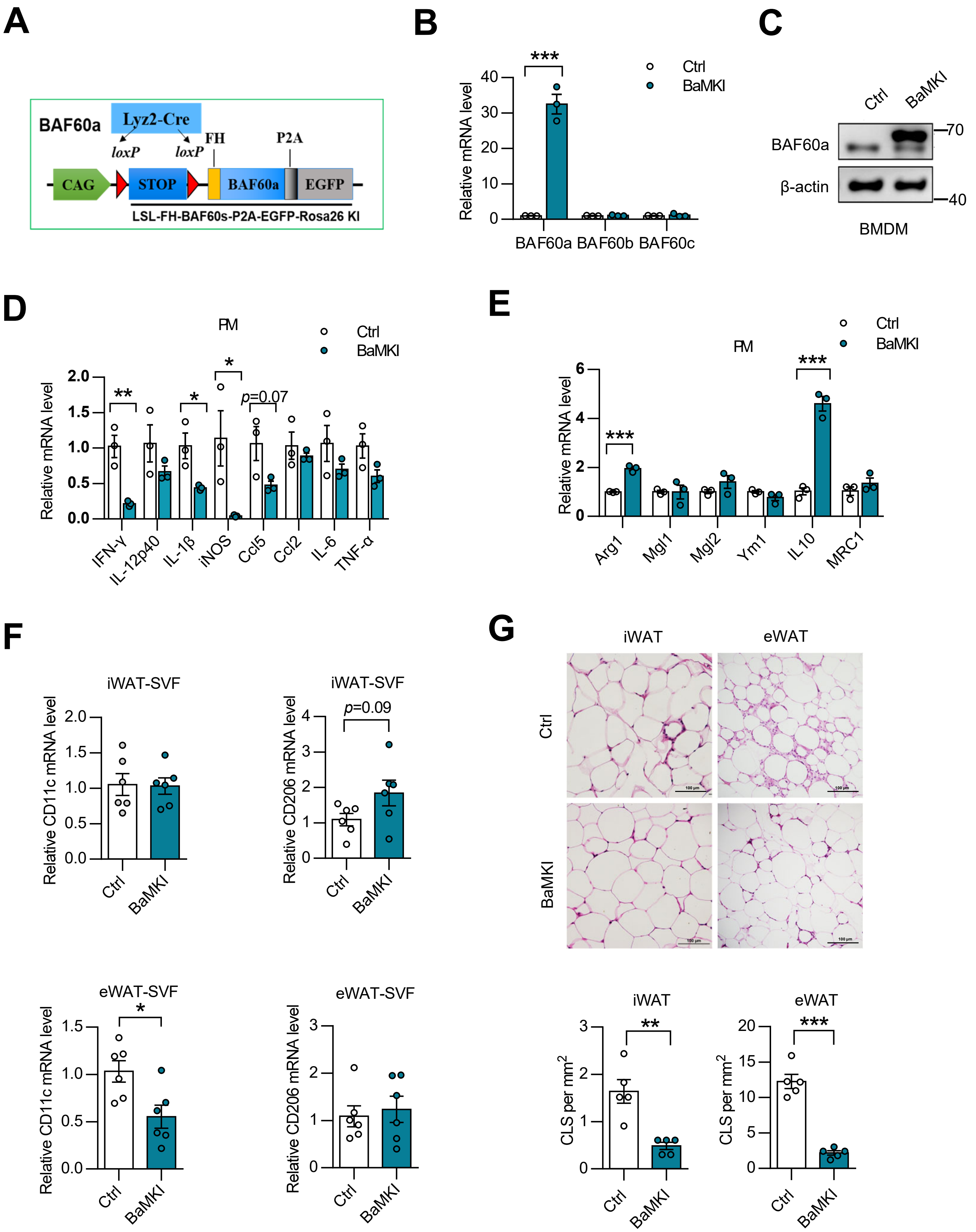

A
BAF60a
Lyz2-Cre
loxP
loxP
FH
P2A
CAG
STOP
BAF60a
EGFP
LSL-FH-BAF60s-P2A-EGFP-Rosa26 KI
B
***
Ctrl
BaMKI
Relative mRNA level
BAF60a BAF60b BAF60c
C
Ctrl
BaMKI
BAF60a
β-actin
70
40
BMDM
D
PM
Ctrl
BaMKI
Relative mRNA level
**
*
*
p=0.07
IFN-γ
IL-12p40
IL-1β
iNOS
Ccl5
Ccl2
IL-6
TNF-α
E
PM
Ctrl
BaMKI
Relative mRNA level
***
***
Arg1
Mgl1
Mgl2
Ym1
IL10
MRC1
F
iWAT-SVF
Relative CD11c mRNA level
Ctrl
BaMKI
iWAT-SVF
Relative CD206 mRNA level
p=0.09
eWAT-SVF
Relative CD11c mRNA level
*
eWAT-SVF
Relative CD206 mRNA level
G
iWAT
eWAT
Ctrl
BaMKI
iWAT
CLS per mm2
**
eWAT
***

Supplementary Fig. 5. Myeloid-specific BAF60a overexpression inhibits proinflammatory macrophage activation.

(**A-C**) Generation and characterization of myeloid-specific BAF60a overexpression (BaMKI) mice. Schematic diagram of the strategy to generate myeloid-BAF60a overexpression mice (**A**); qPCR (n = 3) (**B**) and immunoblotting (**C**) analyses of BAF60a, b, c mRNA and BAF60a protein expression in BMDMs obtained from control and BaMKI mice. (**D**) qPCR analysis of the pro-inflammatory genes in PM from control and BaMKI mice treated with LPS (100 ng/ml) for 4 h (n = 3). (**E**) qPCR analysis of the M2-like macrophage anti-inflammatory genes in PM from control and BaMKI mice treated with IL-4 (20 ng/ml) for 24 h (n = 3). **(F)** qPCR analysis of the CD11c and CD206 mRNA expression in SVFs from the iWAT and eWAT in control and BaMKI mice (n = 6). **(G)** Representative H&E staining images of iWAT and eWAT sections from control and BaMKI mice fed with HFD for 16 weeks. Scale bars, 100 μm. Data represent mean ± SEM. *$P < 0.05$, **$P < 0.01$, and ***$P < 0.001$; ns, no significance.

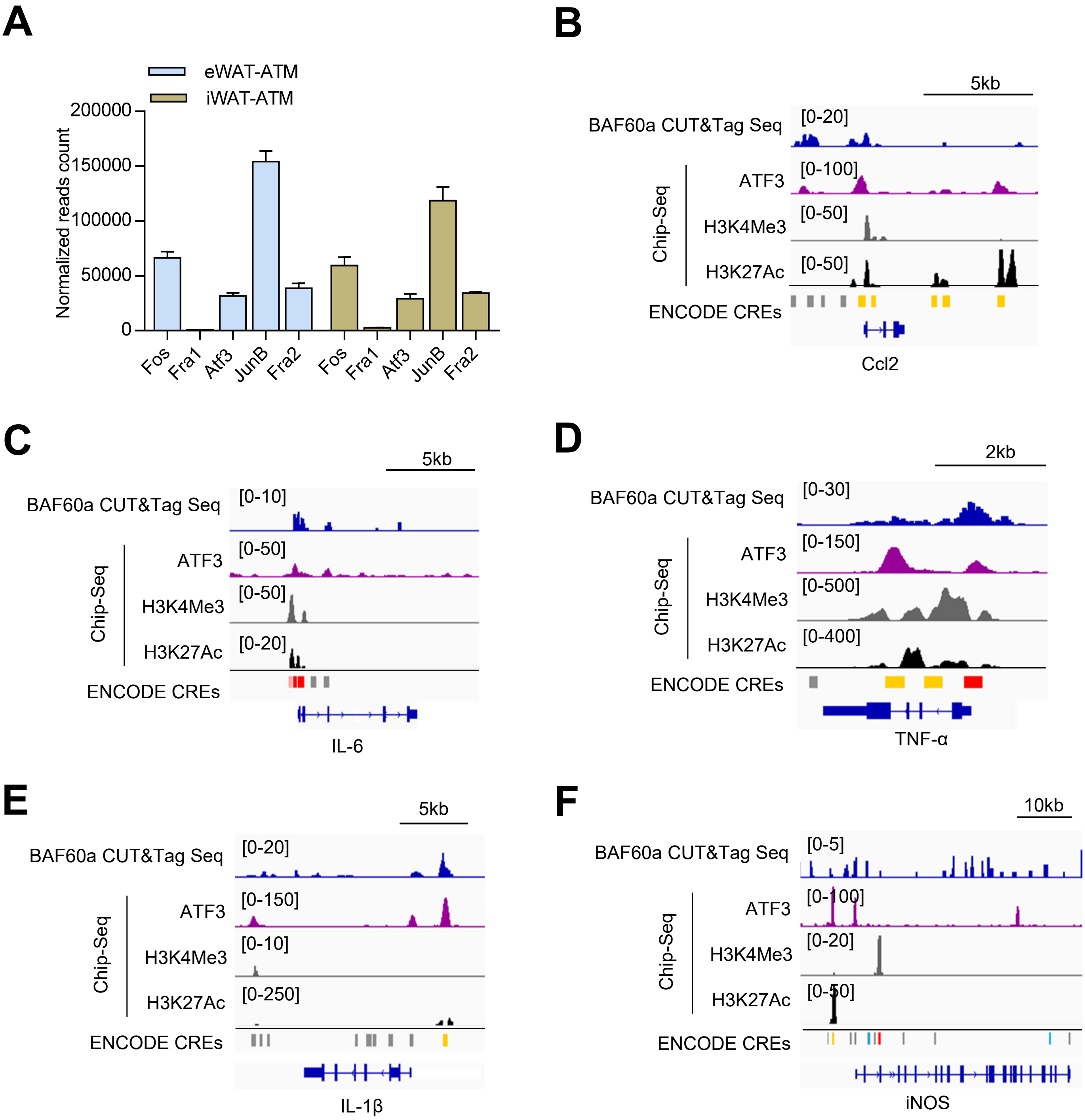

Supplementary Fig. 6. Binding profiles of BAF60a and Atf3 to the genome loci of proinflammatory genes.
(A) Gene expression levels of the indicated transcriptional factors in ATM (F4/80+ cells) from eWAT-SVF cells and iWAT-SVF cells of WT control mice as revealed by RNA-Seq. (B-F) Genome browser tracks of CUT&Tag-Seq (BAF60a) and ChIP-Seq (Atf3, H3K4Me3 and H3K27Ac) data in the genomic loci of BAF60a-regulated proinflammatory genes including Ccl2 (B), IL-6 (C) and TNF-α (D), IL-1β (E), iNOS (F). The ChIP-Seq of H3K4Me3 and H3K27Ac were obtained from ENCODE Database.

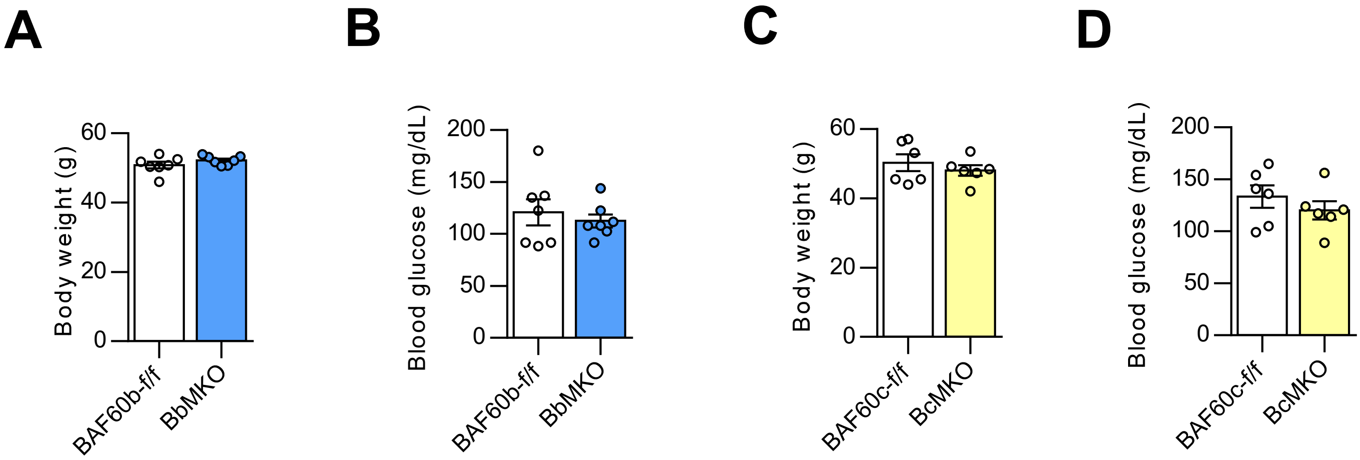

Supplementary Fig. 7. Myeloid-specific inactivation of BAF60b and BAF60c in mice exhibited mild effects on diet-induced obesity and glucose homeostasis.
(**A-B**) Body weight (**A**) and fasting blood glucose levels (**B**) in HFD-fed BAF60b-f/f and BAF60b-f/f-Lyz2-Cre (BbMKO) mice (n = 7). (**C-D**) Body weight (**C**) and fasting blood glucose levels (**D**) in HFD-fed BAF60c-f/f and BAF60c-f/f-Lyz2-Cre (BcMKO) mice (n = 6). Mice were fed with HFD for 8 weeks prior to tissue dissection and analysis. Data represent mean ± SEM. ns, no significance.

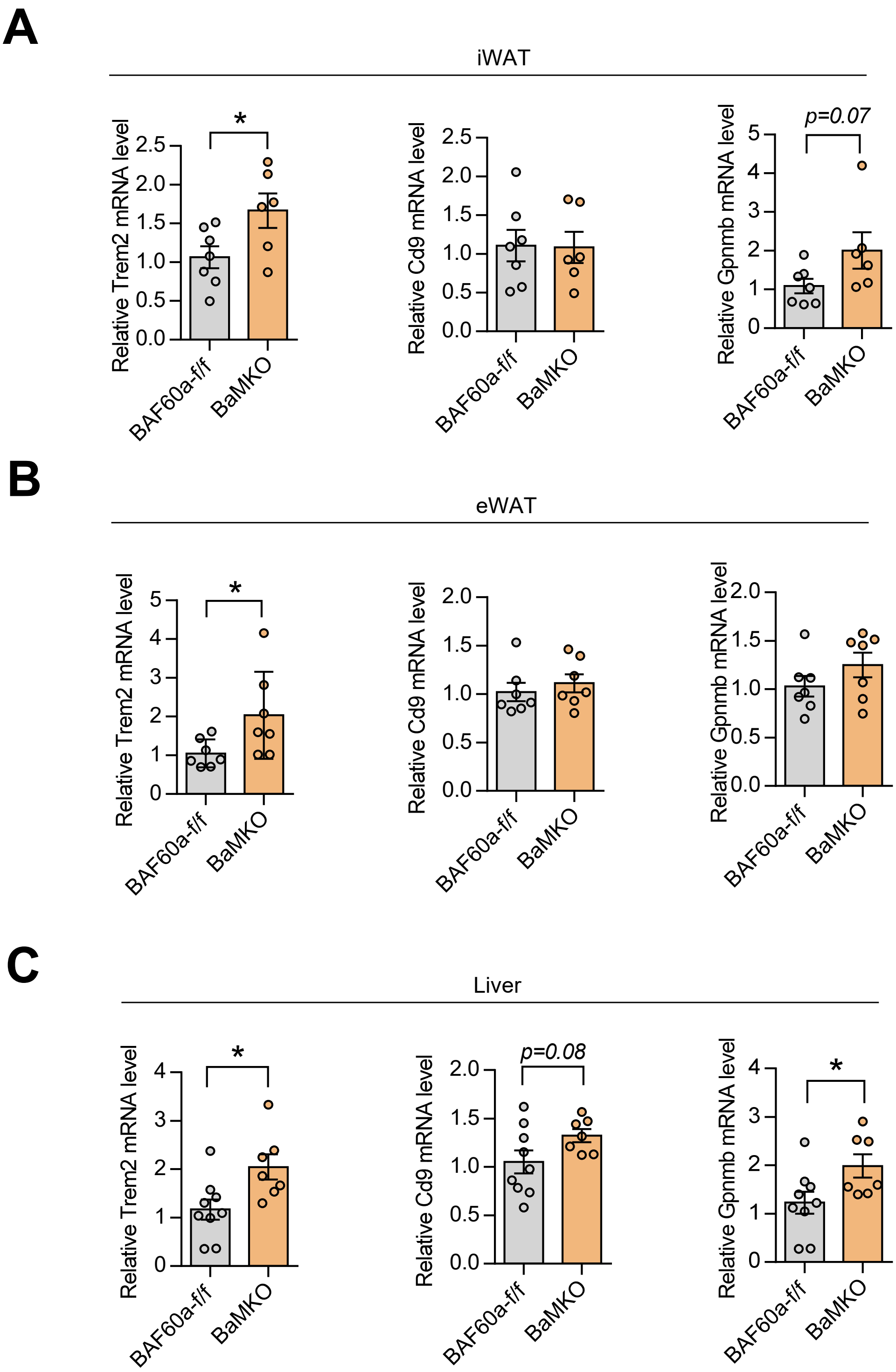

Supplementary Fig. 8. Gene expression analysis of Trem2, Cd9 and Gpnmb in adipose tissues and liver from HFD-fed control and BaMKO mice.

(A-C) qPCR analysis of Trem2, Cd9 and Gpnmb mRNA expression in iWAT (**A**), eWAT (**B**) and liver (**C**) of control and BaMKO mice fed with HFD for 16 weeks (n = 6-9). Data represent mean ± SEM. *$P < 0.05$.

Supplementary Table 1.

Genes	Primers 5' to 3'
BAF60a-F	TGGACCCAAATGACCAGAAAA
BAF60a-R	TCTTGTTGTCTAGAGTGGCGATCT
BAF60b-F	GAAGCTGGACCAGACCATCG
BAF60b-R	CGCAGTTCCCGCATTATCTC
BAF60c-F	AGGCTTACATGGACCTCCTAG
BAF60c-R	CATCAGAGTCTTCCGCATCAG
Nrg4-F	CCCAGCCCATTCTGTAGGTG
Nrg4-R	ACCACGAAAGCTGCCGACAG
Adiponectin-F	GCCCAGTCATGCCGAAGATGAC
Adiponectin-R	AGTGCCATCTCTGCCATCACGG
PPARγ2-F	GAATGCGAGTGGTCTTCCAT
PPARγ2-R	TGCACTGCCTATGAGCACTT
CEBPα-F	AGACATCAGCGCCTACATCGAC
CEBPα-R	GGGTAGTCAAAGTCACCGCCGC
CEBPβ-F	CAAGCTGAGCGACGAGTACA
CEBPβ-R	CAGCTGCTCCACCTTCTTCT
Leptin-F	GAGACCCCTGTGTCGGTTC
Leptin-R	CTGCGTGTGTGAAATGTCATTG
Retn-F	ACAAGACTTCAACTCCCTGTTTC
Retn-R	TTTCTTCACGAATGTCCCACG
Zfp521-F	GGCTGTTCAAACACAAGCG
Zfp521-R	GCACATTTATATGGCTTGTTG
Dlk1-F	GCTGGGACGGGAAATTCTGCGA
Dlk1-R	AACCCAGGTGTGCAGGAGCA
iNOS-F	GAGGCCCAGGAGGAGAGAGATCCG
iNOS-R	TCCATGCAGACAACCTTGGTGTTG
Ccl2-F	AGGTCCCTGTCATGCTTCTG
Ccl2-R	TCTGGACCCATTCCTTCTTG
Ccl5-F	TGCCCACGTCAAGGAGTATTT
Ccl5-R	TTCTCTGGGTTGGCACACACT
F4/80-F	ACCACAATACCTACATGCACC
F4/80-R	AAGCAGGCGAGGAAAAGATAG
IL6-F	AGTTGCCTTCTTGGGACTGA
IL6-R	TCCACGATTTCCCAGAGAAC
TNFα-F	AGCCCCCAGTCTGTATCCTT
TNFα-R	CTCCCTTTGCAGAACTCAGG
IL1β-F	TGGCAACTGTTCCTGAACTCAA
IL1β-R	AGCAGCCCTTCATCTTTTGG
IL12p40-F	CCAGAGACATGGAGTCATAG
IL12p40-R	AGATGTGAGTGGCTCAGAGT
IFNγ-F	TCAAGTGGCATAGATGTGGAAGAA
IFNγ-R	TGGCTCTGCAGGATTTTCATG
CD11c-F	AAAATCTCCAACCCATGCTG
CD11c-R	CACCACCAGGGTCTTCAAGT
MRC1-F	CTCTGTTCAGCTATTGGACGC
MRC1-R	CGGAATTTCTGGGATTCAGCTTC

Mgl1-F	ATGATGTCTGCCAGAGAACC
Mgl1-R	ATCACAGATTTCAGCAACCTTA
Mgl2-F	CAGAACTTGGAGCGGGAAGAG
Mgl2-R	TTCTTGTCACCATTTCTCATCTCCT
IL10-F	GCCAAGCCTTATCGGAAATG
IL10-R	CACCCAGGGAATTCAAATGC
Ym1-F	GGGCATACCTTTATCCTGAG
Ym1-R	CCACTGAAGTCATCCATGTC
Arg1-F	ACACGGCAGTGGCTTTAACC
Arg1-R	TGGCGCATTCACAGTCACTT
Atf3-F	ATAAACACCTCTGCCATCGG
Atf3-R	GCCTCCTTTTCCTCTCATCTTC
36B4-F	GAAACTGCTGCCTCACATCCG
36B4-R	GCTGGCACAGTGACCTCACACG